



NIH PUBLIC ACCESS

Author Manuscript

Virology. Author manuscript; available in PMC 2012 September 1.

Published in final edited form as:

Virology. 2011 September 1; 417(2): 327–333. doi:10.1016/j.virol.2011.06.009.

AAV-6 mediated efficient transduction of mouse lower airways

Wuping Li^{1,5}, Liqun Zhang², Zhijian Wu¹, Raymond J. Pickles^{2,4}, and R. Jude Samulski^{1,3,*}¹Gene Therapy Center, University of North Carolina at Chapel Hill, NC 27599²Cystic Fibrosis/Pulmonary Research and Treatment Center, University of North Carolina at Chapel Hill, NC 27599³Department of Pharmacology, University of North Carolina at Chapel Hill, NC 27599⁴Department of Microbiology and Immunology, University of North Carolina at Chapel Hill, NC 27599⁵The Institute of Blood Transfusion at Chengdu and State Key Laboratory for Molecular Virology and Genetic Engineering, Institute of Pathogen Biology at Beijing, Chinese Academy of Medical Sciences, China. 100730

Abstract

AAV1 and AAV6 are two closely related AAV serotypes. In the present study, we found AAV6 was more efficient in transducing mouse lower airway epithelia *in vitro* and *in vivo* than AAV1. To further explore the mechanism of this difference, we found that significantly more AAV1 bound to mouse airway epithelia than AAV6, yet transduction by AAV6 was far superior. Lectin competition assays demonstrated that both AAV1 and AAV6 similarly utilize α -2, 3-, and to a lesser extent α -2, 6- linked sialic acids as the receptors for transduction. Furthermore, the rates of AAV endocytosis could not account for the transduction differences of AAV1 and AAV6. Finally, it was revealed that AAV6 was less susceptible to ubiquitin/proteasome-mediated blocks than AAV1 when transducing mouse airway epithelia. Thus compared with AAV1, AAV6 has a unique ability to escape proteasome-mediated degradation, which is likely responsible for its higher transduction efficiency in mouse airway epithelium.

Introduction

AAV is a non-pathogenic human parvovirus with a single-stranded DNA genome of 4.7 kb encapsidated in an icosahedral protein shell of ~ 25 nm in diameter (Berns and Giraud, 1996). Following the establishment of the first recombinant clone of AAV serotype 2 (AAV2) in 1982 (Samulski et al., 1983), AAV2 vectors have rapidly gained popularity in gene therapy applications, thanks to their low pathogenicity, the ability to transduce non-dividing cells, and the ability to establish long-term transgene expression. However, clinical applications of AAV vectors (Berns and Giraud, 1996; Ding et al., 2005; Samulski et al., 1983) have been impeded by its restricted cell/tissue tropism, low efficiency of *in vivo* gene delivery, delayed onset of gene expression, and prevalent pre-existing neutralizing

© 2011 Elsevier Inc. All rights reserved.

Corresponding Author: R. Jude Samulski, CB # 7352, Gene Therapy Center, 7113 Thurston Building, The University of North Carolina at Chapel Hill, Chapel Hill, NC 27599-7352, Tel. No: 919-962-3285, Fax No: 919-966-0907, rjs@med.unc.edu.

Publisher's Disclaimer: This is a PDF file of an unedited manuscript that has been accepted for publication. As a service to our customers we are providing this early version of the manuscript. The manuscript will undergo copyediting, typesetting, and review of the resulting proof before it is published in its final citable form. Please note that during the production process errors may be discovered which could affect the content, and all legal disclaimers that apply to the journal pertain.

antibodies in the human populations. Twelve AAV serotypes --AAV1 through 12-- and over one hundred variants have been isolated from tissue samples of human, non-human primates, and other species (Gao, Vandenberghe, and Wilson, 2005; Mori et al., 2004; Schmidt et al., 2008). The tissue tropisms of the different serotypes vary greatly due to the structural diversity of their capsid proteins. The identification of suitable AAV serotypes for specific tissues/cell types is highly desirable and has been pursued intensely in the past decade (Gao, Vandenberghe, and Wilson, 2005; Louboutin, Wang, and Wilson, 2005). Major efforts are focused on modifying capsid proteins to improve the transduction efficiency and/or specificity of AAV-based vectors by rational design and directed evolution (Asokan et al., 2010; Li et al., 2008; Li et al., 2009). The design of tissue-targeted capsid constructs will likely expand and complement the current range of AAV serotypes and variants.

Among all the serotypes, rAAV6 appeared to be a very promising gene delivery vector for the lung. It was isolated as a contaminant of an adenovirus type 5 stock and is now believed to be either a variant of AAV1, with more than 99% amino acid homology between their capsids (Halbert et al., 2000; Rutledge, Halbert, and Russell, 1998), or a natural recombinant between AAV1 and AAV2 (Xiao et al., 1999). It was reported that α -2,3 and α -2,6 sialic acids present on N-linked glycoproteins act as the primary receptors for AAV1 and AAV6 in multiple cell types by mediating viral attachment and infection (Wu et al., 2006b). AAV6 vectors have been shown to mediate higher *in vivo* transduction in the lung (Halbert, Allen, and Miller, 2001), skeletal muscle (Blankinship et al., 2004), and liver (Wu et al., 2006a) than AAV2 or AAV1 vectors. Gregorevic et al. reported that systemic intravenous administration of high dose AAV6 vectors transduced cardiac and skeletal muscle efficiently in mice (Blankinship et al., 2004). Kawamoto S et al. demonstrated the significant potential of AAV6 serotype vectors for early gene expression and widespread regional transduction in myocardium (Kawamoto et al., 2005). These results suggest that AAV6 is a promising vector for gene delivery *in vivo*. However, the mechanism for the enhanced transduction of AAV6 in these tissues has not yet been elucidated.

The effectiveness of rAAVs in gene delivery can be blocked at any of the steps, including the physical binding to the target cells, receptor-mediated endocytosis, vesicular trafficking, endosomal escape, and nuclear import, etc.. Understanding the key step(s) hindering AAV transduction will aid in establishing methods to improve the efficiency of rAAV-mediated gene delivery. In the present study, we have examined these steps in AAV6 mediated transduction of mouse airway epithelia and have found that AAV6 is gifted with the unique ability to escape the proteasome degradation pathway, which is responsible for its superior transduction efficiency in mouse airways.

Results and discussion

AAV6 mediates efficient apical transduction in mouse airway epithelium *in vitro*

We have previously reported that the closely related AAV serotypes AAV1 and AAV6 were able to transduce human airway epithelial cells (HAE) at higher efficiency than other natural serotypes tested (Li et al., 2009). Here we compared their transduction efficiency on HAE and on differentiated mouse airway epithelia (MAE) side by side with AAV1 and AAV6 packaging double strand GFP (AAV1GFP and AAV6GFP). AAV vectors were inoculated to the apical surfaces of HAE/MAE at a dose of 1×10^{11} vg per culture (as optimized in the previous study), and GFP transgene expressions were monitored over time. The numbers of GFP-positive cells were found to reach maximum at 1 week post inoculation (p.i.) and representative epifluorescence images are shown in Fig. 1a. Consistent with our previous data, AAV6 showed higher transduction efficiency than AAV1 on HAE. Surprisingly, AAV6 transduced significantly more cells on MAE than on HAE, i.e., about 30–50% for

MAE to about 1–2% for HAE. AAV1 also transduced more cells on MAE (~5%) than on HAE (<1%), although much less than AAV6. These results suggest that human and mouse airway epithelia are very different in their susceptibility to AAV transduction from the apical surface, and that different AAV vectors may be required for optimal gene transfer in human or mouse airways. The finding is consistent with previous reports that the efficiencies of different AAV serotypes on murine airways were not predictive of their efficiencies on human airways (Flotte et al., 2009; Liu et al., 2006). To determine the cell types targeted by AAV vectors in MAE, the transduced MAE cultures were immunolabeled with a cilia specific marker (β -tubulin IV) followed by optical x-z confocal microscopy. As shown in Figure 1b, both AAV1 and AAV6 transduced only lumen-facing columnar epithelial cells including both ciliated and non-ciliated cells. Although the numbers of cells transduced by AAV1 and AAV6 were different, their cellular tropism was similar. In addition, we quantified the GFP mRNA levels in AAV transduced MAE by quantitative RT-PCR (Fig. 1c). At one month p.i., the GFP mRNA level in AAV6 transduced MAE was approximately one log higher than that by AAV1, consistent with the GFP fluorescence data (Fig. 1a). The levels of GFP mRNA at 2 months p.i. were slightly lower than those at 1 month, confirming that AAV transduction in MAE is relatively stable.

To validate these results with AAV vectors containing double strand GFP transgene, we next tested AAV vectors expressing a single strand luciferase transgene (AAV1luc and AAV6luc). Both the apical or basolateral surfaces of MAE were inoculated with AAV1luc or AAV6luc at 1×10^9 vg, and luciferase enzyme activities were measured at 2 weeks p.i. (Fig. 1d). Not surprisingly, transductions of both viruses from the basolateral surface were about 30 fold higher than that from the apical membrane, even though AAV1 is reported to transduce HAE from both surfaces equally (Yan et al., 2006). Consistent with the findings for GFP-expressing vectors, the transduction efficiency of AAV6 is approximately one Log higher than that of AAV1 from apical surface, likely due to the increased numbers of cells targeted by AAV6.

AAV6 mediates efficient luminal transduction in mouse airways and distal lungs in vivo

To investigate the transduction efficiency of AAV1 and AAV6 in mouse lower airways and distal lungs *in vivo*, a single dose of 1×10^{11} vg/mouse of AAV1GFP or AAV6GFP expressing GFP were inoculated intratracheally in four mice per virus group. Mouse trachea and lungs were harvested at one month p.i.; tissue sections were immuno-labeled with GFP specific antibody to identify AAV transduced cells (green) with cell nuclei labeled with DAPI (blue). Immunohistochemical analyses of mouse lungs for GFP expression revealed that these two AAV vectors demonstrated similar targeting patterns of transduction for conducting airway and alveolar epithelium though with different degrees of efficiency. Representative photomicrographs of the tracheal, bronchiolus, and alveolar regions were shown in Fig. 2a. Tissue sections were processed and are representative of four mice (Fig. 2a). A, B, C are AAV1 mediated GFP expression in alveoli, bronchiolus, trachea respectively and D, E, F are AAV6 mediated GFP expression in alveoli, bronchiolus, trachea respectively—As shown in Fig 2b, quantitation of the number of cells of the alveoli, bronchiolus, trachea expressing GFP indicated that the transduction efficiency of AAV6 and AAV1 of airway epithelia was significant different. AAV6 appears more efficient than AAV1 in the airways. Both vectors showed similar efficiency in transducing both alveoli, bronchiolus. In addition, both vectors were detected with much less frequently in the trachea than in alveoli and bronchiolus. However, AAV6 demonstrated higher efficiency in the trachea than AAV1.

Sialic acid mediates AAV1&6 transduction in MAE, but can not account for the differences in transduction efficiencies between AAV1 than AAV6

To elucidate the mechanisms responsible for the different transduction efficiencies between AAV1 and AAV6, we first determined the binding properties of AAV on the apical surface of HAE and MAE cultures. 5×10^{10} vg/culture (1.0 cm^2) of AAV1 or AAV6 was incubated on the apical surface of HAE or MAE for 2 hrs at 4 C. Unbound viruses were removed followed by three washes with ice-cold DMEM. The numbers of AAV particles bound to the epithelia were harvested and quantified with dot-blot assays (Fig. 3a). Densitometry analysis (Fig. 3b) revealed that more AAV6 bound to HAE membrane than AAV1, consistent with the finding that AAV6 transduced HAE better than AAV1 (Fig. 1a). However, in contrast to the transduction data, the binding of AAV1 on MAE was significantly more than AAV6 (~3 times more), suggesting that AAV virus binding to target cells (i.e., MAE) is not proportional to virus transduction. In another word, the increased transduction of AAV6 than AAV1 is not due to the increased vector binding to MAE (the opposite is true). This notion was further supported by the fact that AAV6 binds both HAE and MAE equally, yet transduced MAE more than a log better than HAE. Therefore, the downstream steps must be responsible for the difference in transduction efficiency between AAV1 and AAV6.

Since both AAV1 and AAV6 use α -2,3 and α -2,6 linked sialic acid as cellular receptors for binding and transduction in non-polarized cells (Wu et al., 2006b), we examined the types and distributions of sialic acids on the apical membrane of HAE and MAE using lectin binding assays. Fluorescence (FITC) labeled sialic acid specific lectins, namely wheat germ agglutinin (WGA, recognizes both α -2,3 and α -2,6 linked sialic acid), maackia amurensis lectin (MAA, recognizes α -2,3-linked sialic acid), and sambucus nigra lectin (SNA, recognizes α -2,6-linked sialic acid) were incubated at $10 \mu\text{g/ml}$ on the apical surface of HAE and MAE, followed by three washes with DMEM. Fluorescent lectins bound to the apical membrane were captured *en face* with fluorescence microscopy (Fig. 3c). The bindings of WGA on both HAE and MAE indicated that the apical surfaces of both HAE and MAE are extensively covered with sialic acid residues. Equal amounts of α -2,3 and α -2,6 linked sialic acids are present on HAE (MAA and SNA bindings respectively). However, α 2,3 linked sialic acids appeared to dominate on MAE, similar to mouse airways *in vivo*. Taken together with the AAV virus binding data, we speculate that AAV1 likely binds to α -2,3 linked sialic acids, however, this interaction might not lead to productive transduction.

To determine the roles of sialic acids in AAV mediated transduction of MAE, we carried out a lectin competition assay (Fig. 3d, 3e). AAV-luc vector (2×10^9 gc/culture) in the presence of 100ug/ml WGA, MAA, or SNA were inoculated on MAE, and AAV transduction was assayed by measuring luciferase activity at 2 weeks p.i. (Fig. 3d, 3e). Despite the difference in AAV1 and AAV6 transductions, the degrees of reductions in the transduction efficiencies by lectin competitions were similar between AAV1 and AAV6. WGA, which binds to sialic acids of both α -2,3 and α -2,6 linkages, inhibited approximately 80% of the transductions for both AAV1 and AAV6, suggesting that AAV1&6 transduction on MAE is mostly sialic acid-dependent. MAA (α -2, 3-specific) blocked ~30% of transduction, whereas SNA (α -2,6-specific) only blocked 15% of transduction by both AAV serotypes, likely due to the fact that there are more α -2,3 than α -2,6 linked sialic acids on MAE (Fig.3c). These findings demonstrate that AAV1 and AAV6 can utilize both α -2, 3 and α -2, 6 linked sialic acids as the primary receptors for MAE transduction, and that sialic acids play a major role in AAV mediated transduction in the airways for both AAV1 and AAV6 serotypes. Thus, the requirement for sialic acid cannot possibly account for the differences in transduction efficiencies between AAV1 and AAV6.

Rate of AAV endocytosis can not account for the differences in the transduction efficiency between AAV1 and AAV6 and between apical vs. basolateral inoculations

We next compared the rates of AAV internalization in MAE by measuring the amounts of endocytosed AAV genome numbers using qPCR of Hirt DNA. MAE were inoculated with equal amounts of AAV1-luc and AAV6-luc ($\text{MOI} = 1 \times 10^4$) from either the apical or basolateral side for 2 hrs followed by three washes with DMEM. Hirt DNA was extracted at 24 hr p.i. and the numbers of endocytosed vector genomes were quantified with qPCR (Fig. 4). For both AAV1 and AAV6, there was no difference in endocytosed AAV copies between the apical and basolateral inoculations, which goes against our previous finding that AAV transductions from the basolateral surface were 30-fold higher than from apical membrane (Fig. 1d). Furthermore, more AAV1 genomes were endocytosed than for AAV6, whereas AAV1 transduction as measured by marker gene expressions (i.e., GFP and luciferase) was at least 10-fold lower than that by AAV6. These findings suggest that the difference in AAV vector internalization does not correlate with viral transduction and can not account for the higher transduction efficiency of AAV6 than AAV1 or of basolateral than apical inoculation. Attempts to separate the nuclear and cytoplasmic fractions of MAE were not successful.

AAV6 has a unique ability at escaping the ubiquitin/proteasome degradation pathway in mouse airway epithelia

The ubiquitin/proteasome pathway plays a role in AAV transduction of non-polarized cell lines and differentiated human airway epithelia (Douar et al., 2001; Duan et al., 2000; Yan et al., 2004). Since neither receptor binding nor vector endocytosis was responsible for the enhanced AAV6 transduction over AAV1, we investigated the role of proteasome pathway on AAV1 and AAV6 transduction. Using the same approach with proteasome modulating agents on HAE (Li et al., 2009), MAE was inoculated from either the apical or basolateral surfaces as before with AAV1luc or AAV6luc ($\text{MOI} = 1 \times 10^3$) in the presence or absence of 40 μM proteasome inhibitor N-acetyl-L-leuciny-L-leuciny-L-norleucinal (LLnL), and the luciferase transgene expressions were assessed at 2 week p.i.. For apical transduction, the treatment of LLnL significant increased the transduction efficiency of both AAV1 and AAV6 (Fig. 5a). However, AAV1 transduction was increased by ~5-fold, versus ~2 fold for AAV6. This suggests that AAV6 is less sensitive to proteasomal degradation compared to AAV1. In another word, AAV6 maybe better equipped to escape the proteasome pathway than AAV1.

The same trend holds true for basolateral transduction, except that it is ~30 fold higher than apical transduction (Fig 5b). This suggests that AAV vectors endocytosed from apical or basolateral surfaces were subjected to a common proteasome processing pathway, and that both AAV1 and AAV6 were different in their sensitivity to proteasome degradation. We conclude that AAV6 is unique in its ability to escape proteasome pathway, which is responsible for its increased transduction efficiency in mouse differentiated airway epithelium. Nonetheless, there was still significant enhancement of AAV6-mediated expression in the presence of the proteasome inhibitor LnLL, suggesting that this capsid is not totally resistant. Some or all of the six amino acid differences between AAV1 and AAV6 capsid may be responsible for the interaction with the ubiquitin/proteasome factors, which we are currently investigating.

Material and methods

Viruses and cells

Recombinant AAV vectors containing double stranded GFP (AAV1-GFP and AAV6-GFP) driven by the chicken- β -actin enhancer and CMV promoter or single stranded Luciferase

(AAV1-luc and AAV6-luc)) were produced using the triple plasmid transfection protocol as described and virus titers were determined by dot-blot analysis (Xiao, Li, and Samulski, 1998). *In vitro* cultures of differentiated human airway epithelia (HAE) was generated as described previously (Li et al., 2009) and cultures of differentiated mouse airway (trachea) epithelial cells (MAE) was generated as previously described (You et al., 2002).

Transduction of MAE with Recombinant AAV Vectors

4–6 week-old MAE cultures were inoculated from the apical or basolateral surface with 100 μ l of AAV vectors for two hours. The MOI varied from MOI of 1×10^3 to 1×10^5 , as indicated in the experiments. The proteasome modulating agent, *N*-acetyl-L-leuciny-L-leuciny-L-norleucinal (LLnL) (40 μ M) (Sigma), was mixed with AAV vectors before inoculation when noted. Photomicrographs of transduced GFP-positive cells were acquired using a Leica Leitz DMIRB inverted fluorescence microscope equipped with a cooled-color charge-coupled device digital camera (MicroPublisher; Q-Imaging), and images of five random fields for each MAE culture were captured. Ciliated cells were immunolabeled with a β -Tubulin IV antibody (Sigma-Aldrich), followed by AlexaFluor594 conjugated goat anti-mouse antibody (Invitrogen) as described previously (Zhang L, JV, 2005). Optical x-z fluorescent confocal images were obtained using a Zeiss 510 Meta Laser Scanning Confocal Microscope. In MAE inoculated with luciferase-expressing AAV vectors, luciferase activities were measured using a luminometer (Perkin Elmer Life Sciences, Victor2 1420 Multilabel Counter).

AAV transductions in mouse trachea in vivo

C57BL/6 Mice (Jackson Lab.) were anesthetized with isoflurane and inoculated intratracheally (i.t.) with 1×10^{11} vg/mouse AAV1-GFP or AAV6-GFP in a volume of 50 μ l by tracheal instillation. At 30 days p.i., mice were sacrificed and systemically perfused with PBS. Lung and trachea were removed and fixed in 10% neutral buffered formalin overnight, followed by equilibration in PBS containing 15% sucrose for 48 hr. Fixed tissues were embedded in paraffin and tissue sections (5 m thickness) were subjected to the immunofluorescence assay to identify AAV transduced cells, which were immunolabeled with GFP-specific antibody (Sigma) followed by AlexaFluor568-conjugated secondary antibody (red) (Invitrogen), whereas nuclei were stained blue with DAPI. Photomicrographs of transduced GFP-positive cells were acquired as described previously.

AAV Binding Assays in vitro

AAV1-luc or AAV6-luc were inoculated to either HAE or MAE on the apical surface at 5×10^{10} vg/transwell epithelium (1 cm^2 surface area) at 4 $^{\circ}\text{C}$ for 2 h. Cells were then rinsed 3 times with PBS, and cell-associated AAV viral DNA was extracted by using DNAeasy kit (Invitrogen). DNA samples were blotted onto a nylon membrane (Ambion) and AAV viral DNA was detected with a P^{32} -labeled Luc DNA probe. Viral genome number were quantitated by dot-blot analysis (Xiao, Li, and Samulski, 1998).

Lectin Staining and Competition Assays

Lectin staining of the apical surface of HAE/MAE was performed by incubating the cells with 10 $\mu\text{g/ml}$ FITC-labeled wheat germ agglutinin (WGA), maackia amurensis lectin (MAA), or sambucus nigra lectin (SNA) (Vector Laboratories Inc.). Briefly, cells were chilled to 4 $^{\circ}\text{C}$, and 10 $\mu\text{g/ml}$ lectin diluted in DMEM was added to the apical surface of the epithelial cultures and incubated at 4 $^{\circ}\text{C}$ for 1 hour. Cultures were then rinsed three times with DMEM, and fixed with 4% paraformaldehyde. Fluorescent photomicrographs of cell-bound lectins were captured with a fluorescent microscope as described above. Lectin competition experiments were done by pre-incubating cells with 100 $\mu\text{g/ml}$ of WGA, MAA,

or SNA at 4°C for 1 hour, followed by incubation with AAV6-luc (2×10^9 gc/transwell) in the presence of 100 µg/ml respective lectin at 4°C for 2 hrs. Cultures were then rinsed three times with DMEM at 4°C for 10 minutes each. Luc expression was determined two weeks later with as described previously (Perkin Elmer Life Sciences, Victor2 1420 Multilabel Counter) (Li et al., 2008).

AAV endocytosis Assay

MAE cultures were incubated at the apical or basolateral membrane with AAV1-GFP or AAV6-GFP at the dose of 1×10^{10} gc/transwell for 2 hrs followed by three times of 10 min washing to remove unbound virus. Cultures were returned to incubator for 22 hours to allow AAV endocytosis. Low molecular weight Hirt DNA was extracted from infected cells as described previously (Duan et al., 2000; Yan et al., 2004). The viral genome in the Hirt DNA from endocytosed AAV was assessed by quantitative PCR (qPCR) performed on a LightCycler 480 as previously described (Johnson and Samulski, 2009).

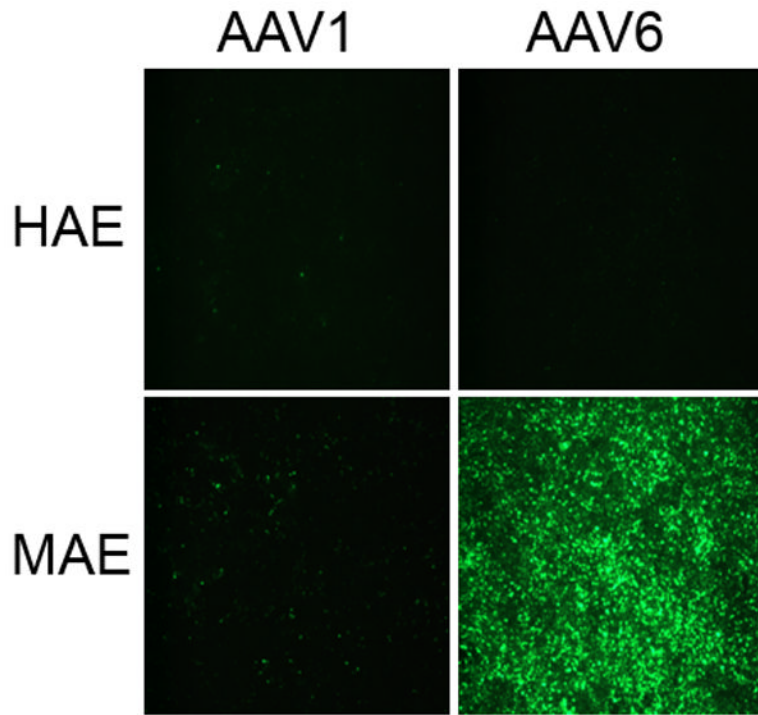
Acknowledgments

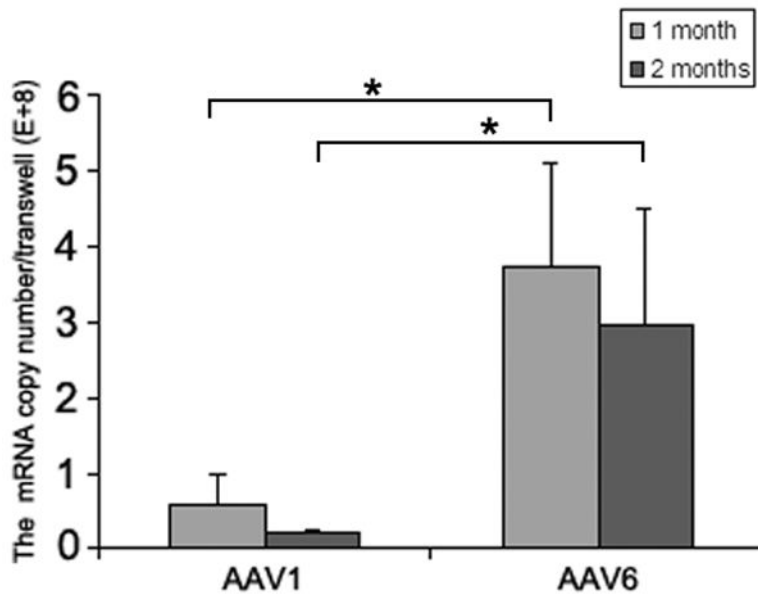
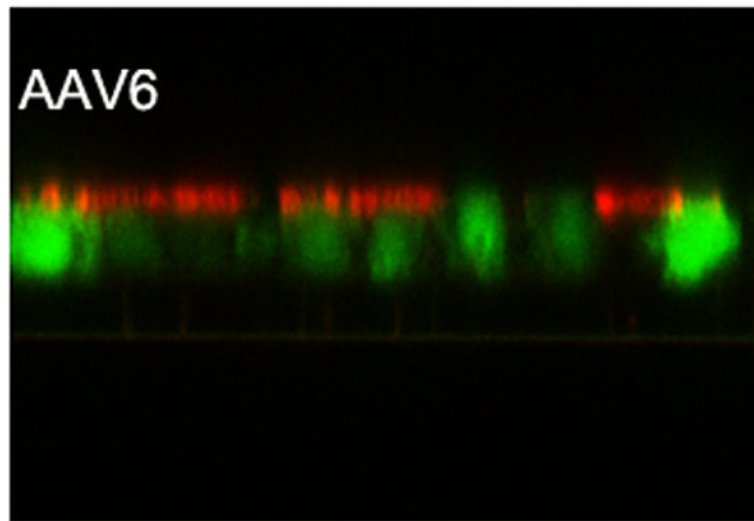
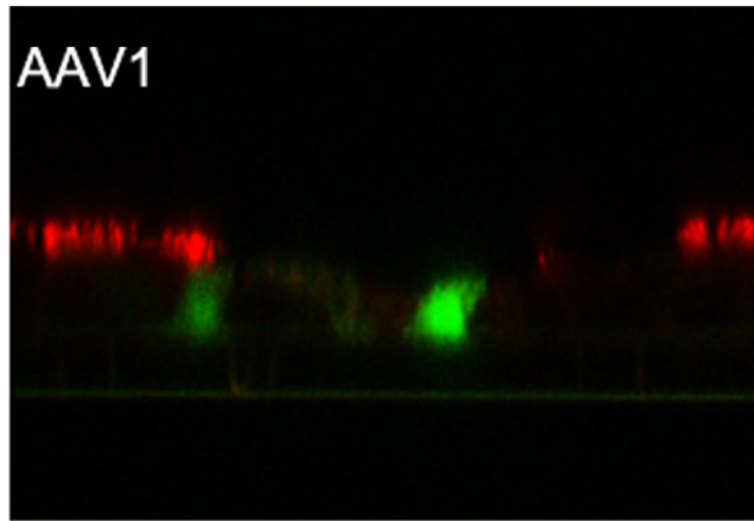
We thank the UNC Cystic Fibrosis Center Tissue Culture Core for providing primary human tracheal epithelial cells and the assistance in generating the mouse airway epithelial cell cultures. This work was supported in part by the Cystic Fibrosis Foundation (Zhang0310) and the National Institutes of Health (R01 HL77844, P01 HL051818, P30 DK065988, P30 DK047757).

References

- Asokan A, Conway JC, Phillips JL, Li C, Hegge J, Sinnott R, Yadav S, DiPrimio N, Nam HJ, Agbandje-McKenna M, McPhee S, Wolff J, Samulski RJ. Reengineering a receptor footprint of adeno-associated virus enables selective and systemic gene transfer to muscle. *Nat Biotechnol.* 2010; 28(1):79–82. [PubMed: 20037580]
- Berns KI, Giraud C. Biology of adeno-associated virus. *Curr Top Microbiol Immunol.* 1996; 218:1–23. [PubMed: 8794242]
- Blankinship MJ, Gregorevic P, Allen JM, Harper SQ, Harper H, Halbert CL, Miller AD, Chamberlain JS. Efficient transduction of skeletal muscle using vectors based on adeno-associated virus serotype 6. *Mol Ther.* 2004; 10(4):671–8. [PubMed: 15451451]
- Ding W, Zhang L, Yan Z, Engelhardt JF. Intracellular trafficking of adeno-associated viral vectors. *Gene Ther.* 2005; 12(11):873–80. [PubMed: 15829993]
- Douar AM, Poulard K, Stockholm D, Danos O. Intracellular trafficking of adeno-associated virus vectors: routing to the late endosomal compartment and proteasome degradation. *J Virol.* 2001; 75(4):1824–33. [PubMed: 11160681]
- Duan D, Yue Y, Yan Z, Yang J, Engelhardt JF. Endosomal processing limits gene transfer to polarized airway epithelia by adeno-associated virus. *J Clin Invest.* 2000; 105(11):1573–87. [PubMed: 10841516]
- Flotte TR, Fischer AC, Goetzmann J, Mueller C, Cebotaru L, Yan Z, Wang L, Wilson JM, Guggino WB, Engelhardt JF. Dual reporter comparative indexing of rAAV pseudotyped vectors in chimpanzee airway. *Mol Ther.* 18(3):594–600. [PubMed: 19826405]
- Gao G, Vandenberghe LH, Wilson JM. New recombinant serotypes of AAV vectors. *Curr Gene Ther.* 2005; 5(3):285–97. [PubMed: 15975006]
- Halbert CL, Allen JM, Miller AD. Adeno-associated virus type 6 (AAV6) vectors mediate efficient transduction of airway epithelial cells in mouse lungs compared to that of AAV2 vectors. *J Virol.* 2001; 75(14):6615–24. [PubMed: 11413329]
- Halbert CL, Rutledge EA, Allen JM, Russell DW, Miller AD. Repeat transduction in the mouse lung by using adeno-associated virus vectors with different serotypes. *J Virol.* 2000; 74(3):1524–32. [PubMed: 10627564]
- Johnson JS, Samulski RJ. Enhancement of adeno-associated virus infection by mobilizing capsids into and out of the nucleolus. *J Virol.* 2009; 83(6):2632–44. [PubMed: 19109385]

- Kawamoto S, Shi Q, Nitta Y, Miyazaki J, Allen MD. Widespread and early myocardial gene expression by adeno-associated virus vector type 6 with a beta-actin hybrid promoter. *Mol Ther*. 2005; 11(6):980–5. [PubMed: 15922969]
- Li W, Asokan A, Wu Z, Van Dyke T, DiPrimio N, Johnson JS, Govindaswamy L, Agbandje-McKenna M, Leightle S, Redmond DE Jr, McCown TJ, Petermann KB, Sharpless NE, Samulski RJ. Engineering and selection of shuffled AAV genomes: a new strategy for producing targeted biological nanoparticles. *Mol Ther*. 2008; 16(7):1252–60. [PubMed: 18500254]
- Li W, Zhang L, Johnson JS, Zhijian W, Grieger JC, Ping-Jie X, Drouin LM, Agbandje-McKenna M, Pickles RJ, Samulski RJ. Generation of novel AAV variants by directed evolution for improved CFTR delivery to human ciliated airway epithelium. *Mol Ther*. 2009; 17(12):2067–77. [PubMed: 19603002]
- Liu X, Yan Z, Luo M, Engelhardt JF. Species-specific differences in mouse and human airway epithelial biology of recombinant adeno-associated virus transduction. *Am J Respir Cell Mol Biol*. 2006; 34(1):56–64. [PubMed: 16195538]
- Louboutin JP, Wang L, Wilson JM. Gene transfer into skeletal muscle using novel AAV serotypes. *J Gene Med*. 2005; 7(4):442–51. [PubMed: 15517544]
- Mori S, Wang L, Takeuchi T, Kanda T. Two novel adeno-associated viruses from cynomolgus monkey: pseudotyping characterization of capsid protein. *Virology*. 2004; 330(2):375–83. [PubMed: 15567432]
- Rutledge EA, Halbert CL, Russell DW. Infectious clones and vectors derived from adeno-associated virus (AAV) serotypes other than AAV type 2. *J Virol*. 1998; 72(1):309–19. [PubMed: 9420229]
- Samulski RJ, Srivastava A, Berns KI, Muzyczka N. Rescue of adeno-associated virus from recombinant plasmids: gene correction within the terminal repeats of AAV. *Cell*. 1983; 33(1):135–43. [PubMed: 6088052]
- Schmidt M, Voutetakis A, Afione S, Zheng C, Mandikian D, Chiorini JA. Adeno-associated virus type 12 (AAV12): a novel AAV serotype with sialic acid- and heparan sulfate proteoglycan-independent transduction activity. *J Virol*. 2008; 82(3):1399–406. [PubMed: 18045941]
- Wu Z, Asokan A, Grieger JC, Govindasamy L, Agbandje-McKenna M, Samulski RJ. Single amino acid changes can influence titer, heparin binding, and tissue tropism in different adeno-associated virus serotypes. *J Virol*. 2006a; 80(22):11393–7. [PubMed: 16943302]
- Wu Z, Miller E, Agbandje-McKenna M, Samulski RJ. Alpha2,3 and alpha2,6 N-linked sialic acids facilitate efficient binding and transduction by adeno-associated virus types 1 and 6. *J Virol*. 2006b; 80(18):9093–103. [PubMed: 16940521]
- Xiao W, Chirmule N, Berta SC, McCullough B, Gao G, Wilson JM. Gene therapy vectors based on adeno-associated virus type 1. *J Virol*. 1999; 73(5):3994–4003. [PubMed: 10196295]
- Xiao X, Li J, Samulski RJ. Production of high-titer recombinant adeno-associated virus vectors in the absence of helper adenovirus. *J Virol*. 1998; 72(3):2224–32. [PubMed: 9499080]
- Yan Z, Lei-Butters DC, Liu X, Zhang Y, Zhang L, Luo M, Zak R, Engelhardt JF. Unique biologic properties of recombinant AAV1 transduction in polarized human airway epithelia. *J Biol Chem*. 2006; 281(40):29684–92. [PubMed: 16899463]
- Yan Z, Zak R, Zhang Y, Ding W, Godwin S, Munson K, Peluso R, Engelhardt JF. Distinct classes of proteasome-modulating agents cooperatively augment recombinant adeno-associated virus type 2 and type 5-mediated transduction from the apical surfaces of human airway epithelia. *J Virol*. 2004; 78(6):2863–74. [PubMed: 14990705]
- You Y, Richer EJ, Huang T, Brody SL. Growth and differentiation of mouse tracheal epithelial cells: selection of a proliferative population. *Am J Physiol Lung Cell Mol Physiol*. 2002; 283(6):L1315–21. [PubMed: 12388377]





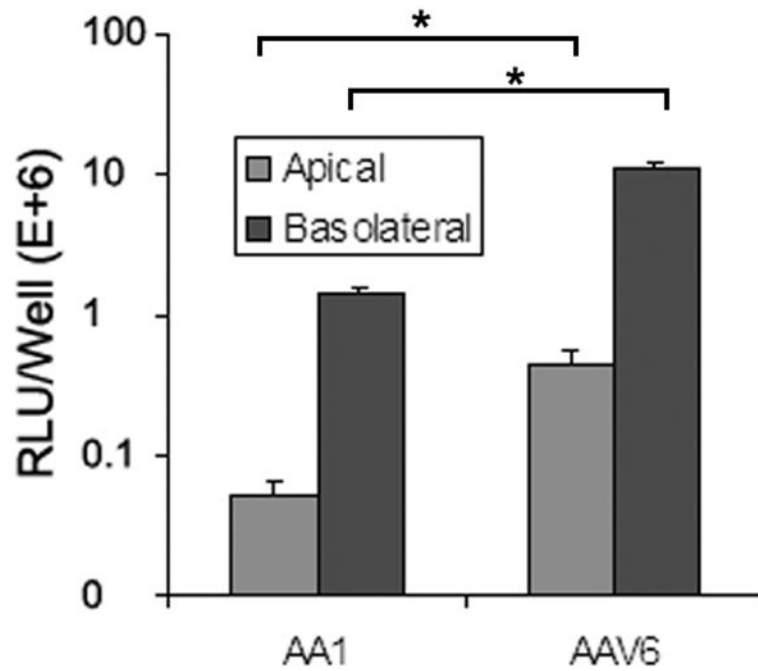


Fig. 1. Transduction efficiencies of AAV1 and AAV6 in human and mouse airway epithelial models *in vitro*

Human and mouse airway epithelial cultures (HAE and MAE respectively) were inoculated apically with AAV1-GFP or AAV6-GFP at a dose of 1×10^{11} vg/culture (1.0 cm^2 surface area) (MOI = 1×10^5). Representative *en face* fluorescence photomicrographs showing GFP-positive cells were obtained at 14 days post inoculation (p.i.). (a) Optical x-z confocal images of MAE transduced with AAV1-GFP and AAV6-GFP showing AAV-transduced cells as GFP positive. Cilia were immunolabeled with β -tubulin IV antibody (red) as described in “Material and Methods”. (b) The apical surface of MAE was inoculated with AAV1-GFP or AAV6-GFP (MOI of 5×10^4). The mRNA from MAE was harvested at 1 and 2 months p.i., and relative GFP mRNA copy numbers were determined with qRT-PCR (as described in “Material and Methods”). Asterisk (*) denotes $P < 0.01$. (c) AAV1-Luc or AAV6-Luc at a dose of 10^9 gc/culture (1 cm^2) was applied to either the apical surface or the basolateral side of MAE and allowed to incubate at 37°C for 2 hrs. At 14 days p.i., luciferase activities were assessed, and presented as the mean (\pm SEM) luciferase activity per cm^2 epithelia (n=4). RLU, relative light units. Asterisk (*) denotes $P < 0.01$.

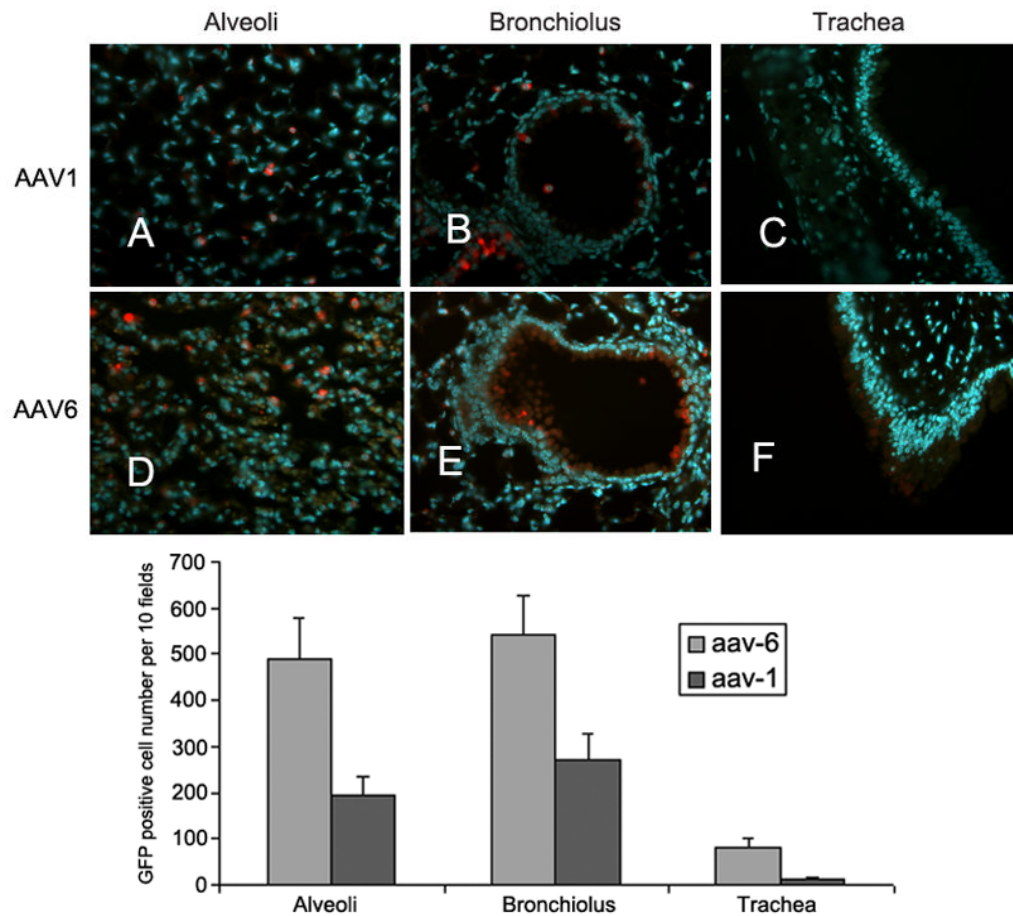
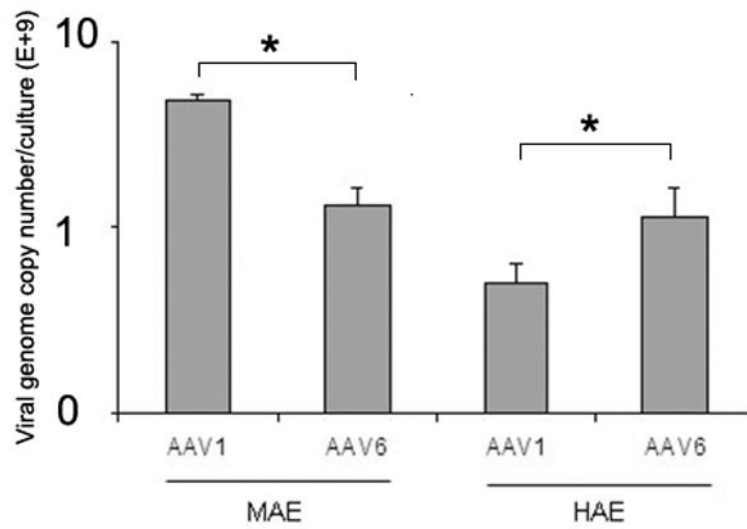
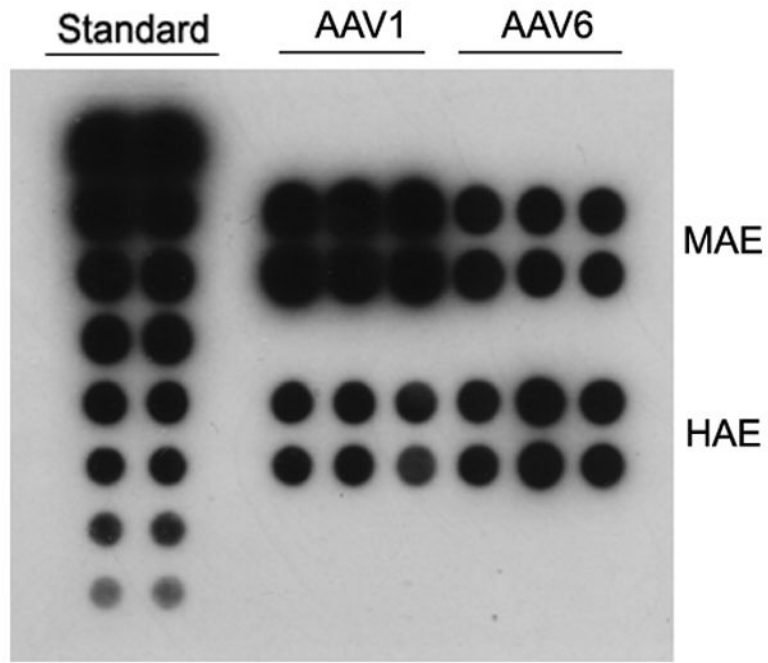


Fig. 2. AAV transduction of mouse airways *in vivo*

(a) Balb/c mice were inoculated by the intro-tracheal route with a single dose of 1×10^{11} vg/mouse in a volume of 50 μ l of AAV1-GFP (panels A, B and C) or AAV6-GFP (D, E, and F). Mouse trachea and lungs were harvested at 1 month p.i.. Paraffin-embedded tissue sections were prepared, and transduced cells were immunolabeled with rabbit anti-GFP antibody (Sigma) followed by Alexafluor594- conjugated goat anti-rabbit antibody (Invitrogen). Nuclei were stained blue with DAPI. Representative images for alveolar (A & D), bronchiolus (B & E), and tracheal regions (C & F) are shown. (b) The numbers of GFP positive cells per image field were quantified and the mean numbers from five random images were shown (\pm SEM).



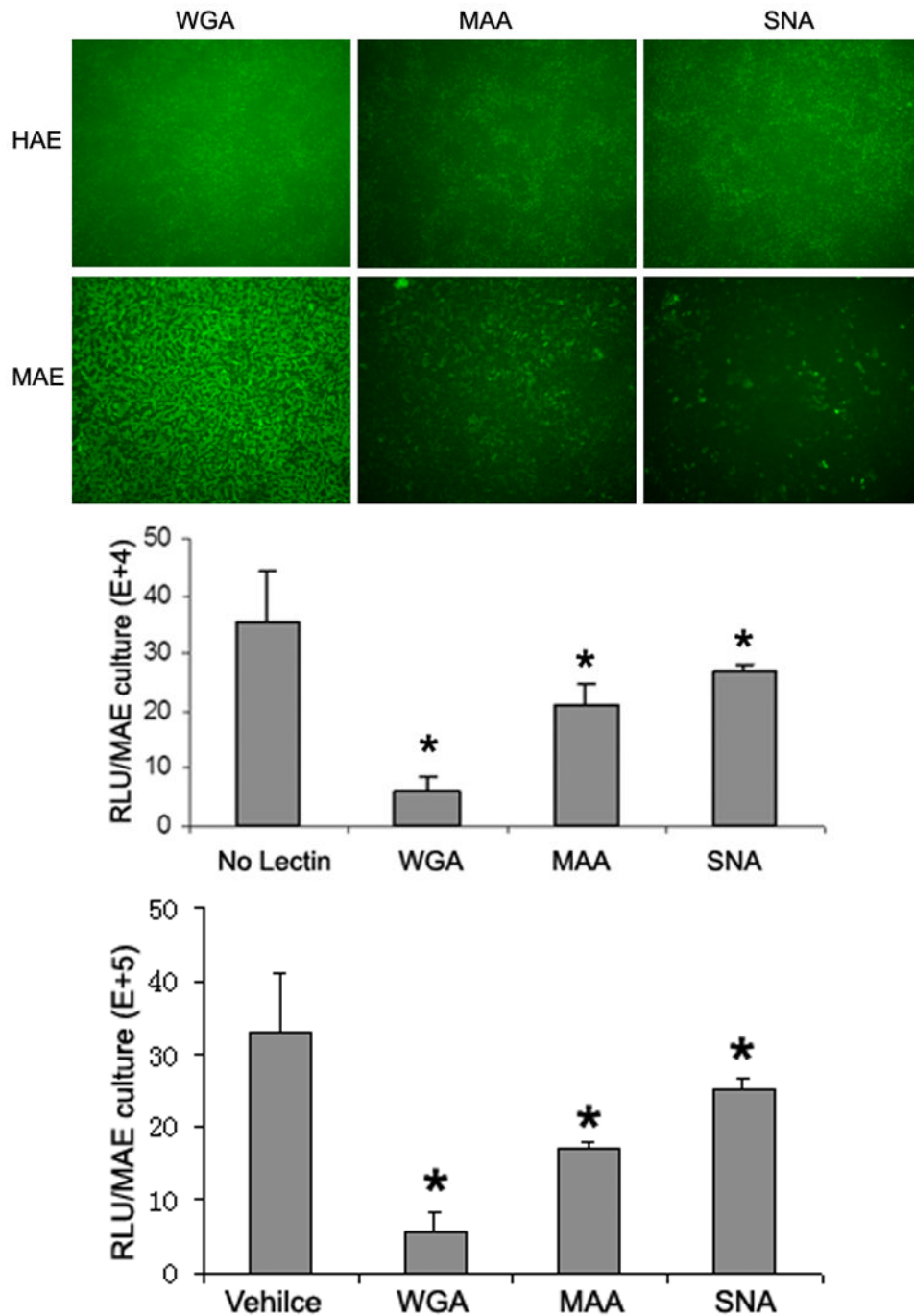


Fig. 3. AAV transductions in HAE/MAE is sialic acid-dependent

(a) Relative AAV bindings to HAE and MAE. AAV1 or AAV6 at a dose of 5×10^{10} vg/culture (cm^2) were allowed to bind to the apical surface of HAE or MAE and incubated at 4 C for one hour. Cell-associated AAV viral DNA was harvested from cell lysate and quantified with dot-blot analysis ($n=6$). Densitometry was performed against a standard and results are shown in (b). (c) The apical surface of HAE and MAE was probed with FITC-labeled selective sialic acid-binding lectins: WGA (sialic acids of both α -2,3 and α 2,6 linkages), MAA (α 2,3-linked sialic acids), and SNA (α 2,6-linked sialic acids) at 10 $\mu\text{g/ml}$

concentration. Representative fluorescent photomicrographs were shown. (d) and (e) Lectin competition assay. MAE cultures were pre-incubated on the apical surface with 100 $\mu\text{g}/\text{ml}$ of each lectin at 4°C for 1 hr. The lectins were then removed, and solutions containing 100 $\mu\text{g}/\text{ml}$ lectin and AAV1-Luc (d) or AAV6-Luc (e) ($\text{MOI} = 2 \times 10^3$) were inoculated. Luciferase assay was performed at 14 days p.i., and the means (\pm SEM) were shown (n=4). RLU, relative light units. Asterisk (*) denotes $P < 0.05$.

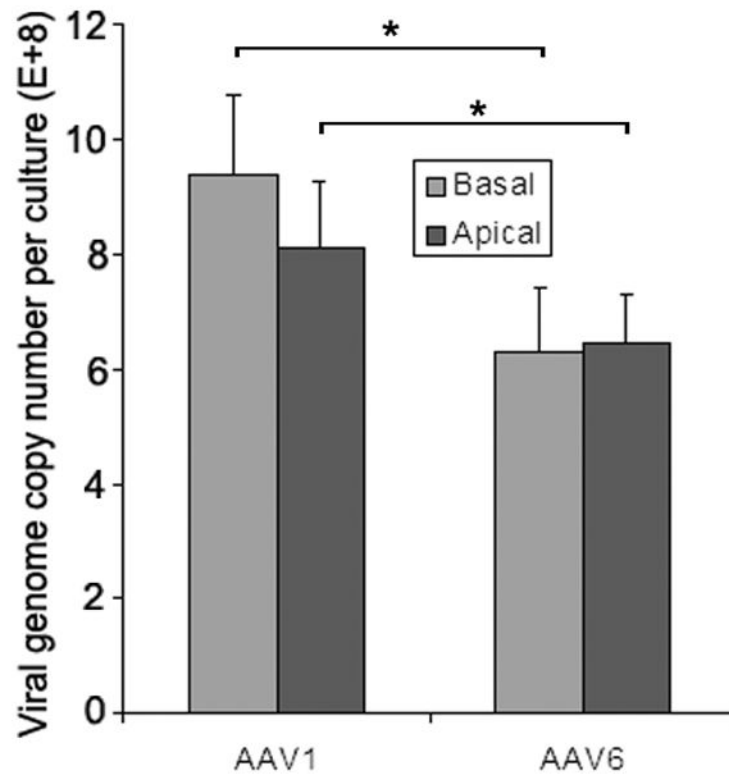


Fig. 4. AAV endocytosis at the apical and basolateral membranes

AAV1 or AAV6 at MOI of 1×10^4 was incubated with the apical or basolateral surfaces of MAE cultures at 37°C for 2 hrs, followed by washing with DMEM three times to remove unbound virus. At 22 hrs p.i., Hirt DNA was extracted from infected cells and viral genome copies were assessed by quantitative PCR (qPCR). Data represent the mean \pm SEM (n=4). Asterisk (*) denotes $P < 0.05$.

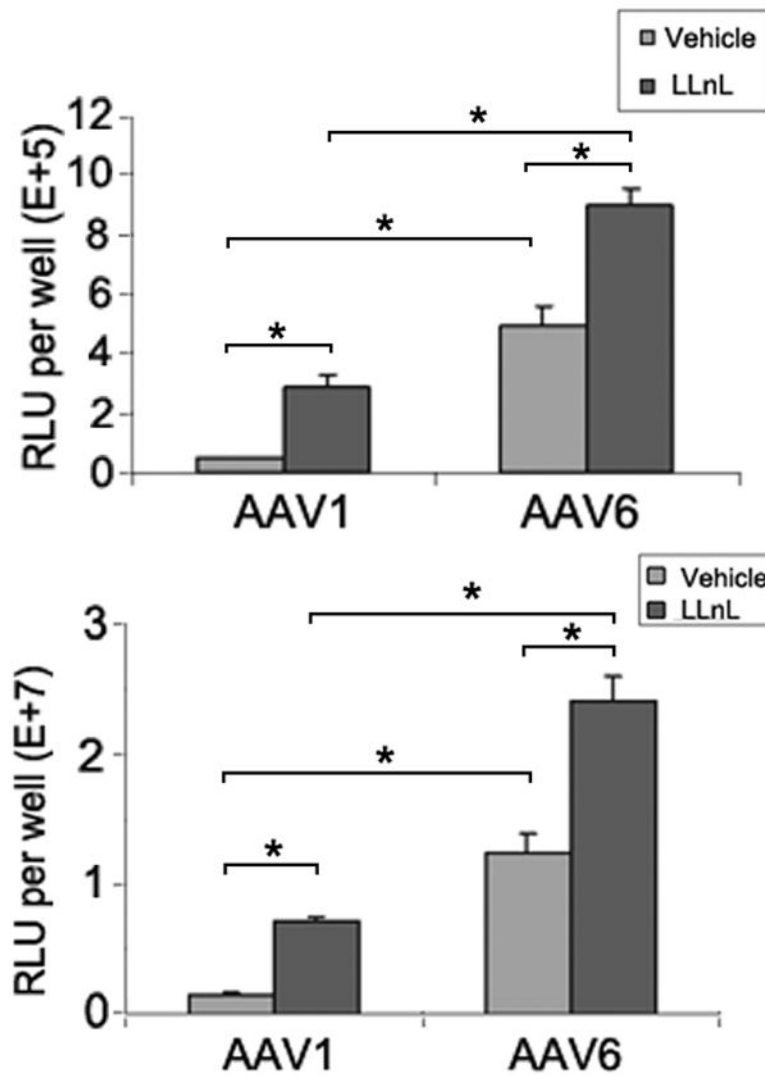


Fig. 5. Effects of proteasome pathway on AAV transduction of MAE
 AAV1-Luc, AAV6-Luc were inoculated on either the apical surface (a) or the basolateral side (b) of MAE cultures ($MOI = 1 \times 10^3$) and incubated for 2 hrs at 37°C in the presence or absence of the proteasome inhibitor LLnL at the concentration of 40 μ M. Relative luciferase activities in relative light units (RLU) were assessed at 2 weeks p.i.. Data represent the mean (\pm SEM) (n=4.). Asterisk (*) denotes $P < 0.05$.